J Sol-Gel Sci Technol (2016) 77:152–159
DOI 10.1007/s10971-015-3839-5

ORIGINAL PAPER

New kinds of hybrid materials containing covalently bonded Tb^{3+} (Eu^{3+}) complexes organically modified titania and alumina network via sol–gel process

Qiang Zhang[1] · Ye Sheng[1] · Keyan Zheng[1] · Haifeng Zou[1]

Received: 20 May 2015 / Accepted: 10 August 2015 / Published online: 2 September 2015

Abstract This work focuses on the construction of a series of novel chemically bonded inorganic–organic rare earth hybrid materials using 3,4-bis(pyridin-4-yl-methoxy)benzoic acid as an organic bridge molecule that can both coordinate with rare earth ions and form an inorganic network with titanium isopropylate and aluminum isopropylate after cohydrolysis and copolycondensation through a sol–gel process. Measurements of the properties of these materials show that the terbium systems present high thermal stability and amorphous structure features. UV excitation in the organic component resulted in strong green emission from Tb^{3+} ions due to an efficient ligand-to-metal energy-transfer mechanism.

Graphical Abstract

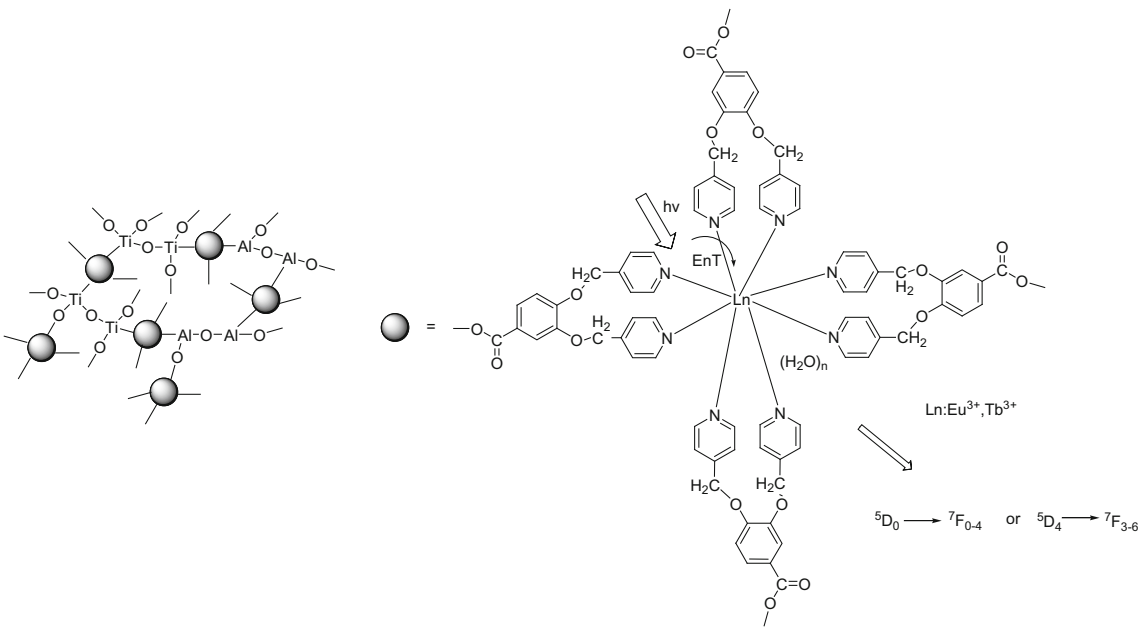

Keywords Lanthanide ions · Organic/inorganic hybrids · Organically modified alumina/titania · Chemical bonding assembly · Photoluminescence · Sol–gel process

✉ Haifeng Zou
haifengzou0431@gmail.com

[1] College of Chemistry, Jilin University, Changchun 130012, People's Republic of China

1 Introduction

Lanthanide ions, especially trivalent terbium and europium, have recently attracted considerable interest in the numerous fields such as full-color display devices, less-harmful labelling reagents, microscopy and luminescent probes, because of their unique line-like emission bands, substantial stokes shifts, very long luminescence lifetimes and so on [1–4]. But direct photoexcitation of lanthanide ions disfavored due to the spin and parity forbidden nature of the *f–f* transitions. Weissman et al. first observed that the use of the organic ligands β-diketone in europium complexes increased the luminescence intensity from the lanthanide ion when such complexes were irradiated with ultraviolet lights. In these systems, the organic ligands act as photosensitizers to absorb and transfer the energy of light to excite the lanthanide ions via an energy-transfer process, which is defined as antenna effect [5, 6]. In this area, most of the previous studies concern the sol–gel approach to synthesize a kind of organic–inorganic materials, which allows mechanically mixing of inorganic and organic components at the predicated scale and under mild temperature processing conditions [7–10]. However, since there are only interactions of hydrogen bonds or van der Waals forces between organic and inorganic parts, this kind of materials presents two separate phases leading to leaching of the complexes and obtaining in-homogenous systems [11–14]. Thus, some work focuses on grafting covalently the organic ligands to the inorganic backbone. The materials were mainly developed for silicate systems so far. For instance, Franville et al. synthesized a series of hybrid materials with different structures in which lanthanide complex luminescent centers were bonded with silica-based matrix through Si–C linkage by hydrolysis and condensation reactions. They found that the complexes containing europium(III) ions in the silica hybrid matrix had a much higher thermal stability than the complex with the organic part alone [15]. The enlargement of the chemistry to metal oxides other than silica would allow interesting new options for the development of inorganic–organic hybrid materials. Aimed at preparing non-silicate hybrid systems such as titania and aluminum hybrid networks, some approaches have been tried. Li et al. took advantage of modification of the titanium alkoxide by the ligand isonicotinic acid to develop new strategies to place lanthanide complex luminescent molecules in desired inorganic titanium framework. The ligands can both react with titanium alkoxide to form an amorphous Ti–O network and act as an antenna to absorb and transfer energy to the lanthanide ions [16]. Cuan et al. prepared alumina and titania xerogels encapsulated with high luminescent lanthanide polyoxometalates via a sol–gel process. These hybrid materials possess favorable luminescent performances, and it is discovered that hybrids of titania gels can be applied in close white-light integration [17].

On the basis of the former work, the key procedure to construct molecular-based materials is to design functional bridge molecule, which both coordinates lanthanide ions and constitutes the covalent organic–inorganic network by sol–gel processing [16–19]. In this work, 3,4-bis(pyridin-4-ylmethoxy)benzoic acid is selected to construct the linkage between inorganic matrix and rare earth ions. The carboxylic acid group of it can react with metallic alkoxide to moderate the reactivity toward hydrolysis and condensation, while the heterocyclic group can coordinate with rare earth ions as well as sensitize the luminescence of them. And the novel Tb^{3+} (Eu^{3+}) luminescent hybrid materials having titania-/alumina-based host were prepared by 3,4-bis(pyridin-4-ylmethoxy)benzoic acid and titanium isopropylate/aluminum isopropylate through the sol–gel method. In addition, structural characterization and detail studies of photophysical properties of the resulting hybrid materials were thoroughly investigated.

2 Experimental

2.1 Materials

Two lanthanide(III) chloride $LnCl_3{\cdot}6H_2O$ (Ln = Tb^{3+}, Eu^{3+}) were prepared by the corresponding oxides (Tb_4O_7, Eu_2O_3) in the laboratory. Titanium isopropylate, aluminum isopropylate, 3,4-dihydroxybenzoic acid and 4-(chloromethyl)pyridine were from Aladdin Industrial Corporation. Concentrated sulfuric acid (98.0 %), hydrochloric acid (37 %), sodium hydroxide, *N*,*N*-dimethylformamide (DMF) and ethanol were purchased from Beijing Chemical Company Limited.

2.2 Synthesis of 3,4-bis(pyridin-4-ylmethoxy)benzoic acid

Four milliliters of concentrated sulfuric acid was added into 200 ml alcoholic solution of 50 mmol 3,4-dihydroxybenzoic acid, and the solution was mixed and refluxed for 6–7 h. The excess ethanol was removed under vacuum, and then, the reaction mixture was poured into ice cold water. The resulting precipitate was filtered off, washed with deionized water and dried. To 10 mmol solid product, 20 mmol 4-pycolyl chloride hydrochloride and 20 mmol sodium hydroxide and 50 ml DMF were added. The mixture was heated at 100 °C for 8 h and then acidified with dilute HCl, and the resulting precipitate was filtered, washed, dried and recrystallized from ethanol. A light brown precipitate was obtained, and the yield was about

65 %. ^{1}H NMR (300 MHz, DMSO): δ (ppm) 8.57 (m, 4H), 7.55 (t, $J = 5.7$ Hz, 1H), 7.46 (m, 5H), 7.13 (d, $J = 8.4$ Hz, 1H), 5.25 (s, 4H). Elemental analyses calcd (%) for $C_{19}H_{16}N_2O_4$ (336.35): C, 67.84; H, 4.81; N, 8.33. Found C, 67.87; H, 4.79; N, 8.32. MS (EI) m/e = 336 (M^+).

2.3 Synthesis of hybrids Ti–PYB–Ln, Al–PYB–Ln and Ti–Al–PYB–Ln (PYB = 3,4-bis(pyridin-4-ylmethoxy)benzoic acid, Ln^{3+} = Tb^{3+}, Eu^{3+})

A typical synthesis procedure of Ti–PYB–Ln was as follows: 4 mmol 3,4-bis(pyridin-4-ylmethoxy)benzoic acid was dissolved in 40 ml DMF, and then, 4 mmol titanium isopropylate was slowly added. After refluxing and stirring for 1 h, 1 mmol $LnCl_3{\cdot}6H_2O$ dissolved in 5 ml DMF was added dropwise into the clear solution and refluxed for 3 h. Finally, 0.2 ml deionized water was dropped into the above solution in order to promote the hydrolysis of titanium isopropylate to form inorganic/organic hydrogels constructed by network. Then, the final materials Ti–PYB–Ln were obtained by centrifugation and washed with ethanol for three times and dried for 24 h at 100 °C. All the other hybrids were synthesized using the same procedure except that Ti–Al–PYB–Ln was prepared using 2 mmol titanium isopropylate and 2 mmol aluminum isopropylate, and Al–PYB–Ln was prepared using 4 mmol aluminum isopropylate.

For Ti–PYB–Eu (%) Anal. Calcd.: C, 44.20; H, 3.03; N, 5.43. Found: C, 44.20; H, 3.00; N, 5.33.

For Ti–PYB–Tb (%) Anal. Calcd.: C, 44.05; H, 3.02; N, 5.41. Found: C, 44.05; H, 2.99; N, 5.30.

For Al–PYB–Eu (%) Anal. Calcd.: C, 47.60; H, 3.26; N, 5.84. Found: C, 47.60; H, 3.15; N, 5.72.

For Al–PYB–Tb (%) Anal. Calcd.: C, 47.43; H, 3.25; N, 5.82. Found: C, C, 47.42; H, 3.17; N, 5.79. For Ti–Al–PYB–Eu (%) Anal. Calcd.: C, 45.84; H, 3.14; N, 5.63. Found: C, 45.84; H, 3.10; N, 5.52.

For Ti–Al–PYB–Tb (%) Anal. Calcd.: C, 45.68; H, 3.13; N, 5.61. Found: C, 45.68; H, 3.07; N, 5.55. In addition, the contents of lanthanide ions (Eu^{3+}, Tb^{3+}) in the hybrids are determined by EDTA titration.

For Ti–PYB–Eu (%) Anal. Calcd.: Eu, 7.36. Found: Eu, 7.33.

For Ti–PYB–Tb (%) Anal. Calcd.: Tb, 7.67. Found: Tb, 7.66.

For Al–PYB–Eu(%) Anal. Calcd.: Eu, 7.92. Found: Eu, 7.63.

For Al–PYB–Tb(%) Anal. Calcd.: Tb, 8.26. Found: Tb, 8.24.

For Ti–Al–PYB–Eu(%) Anal. Calcd.: Eu, 7.63. Found: Eu, 7.53.

For Ti–Al–PYB–Tb(%) Anal. Calcd.: Tb, 7.95. Found: Tb, 7.36.

2.4 Characterization

^{1}H NMR spectra were recorded on a Bruker 510 spectrometer. Fourier transform infrared spectroscopy (FTIR) spectra were checked by Nicolette 5PC FTIR spectrophotometer. Powder X-ray diffraction (XRD) spectra were carried out on a XRD-6000 X-ray diffractometer (Shimadzu) with Cu Kα radiation ($\lambda = 0.15405$ nm) over the range of 10°–70°. Thermogravimetric analysis data were recorded with a thermal analysis instrument (TGA 1600 LF, METTLER TOLEDO, Switzerland) at a heating rate of 10 °C min^{-1} in an N_2 flow. The morphology of the samples was inspected using a scanning electron microscope (SEM, S-4800, Hitachi). Photoluminescence (PL) excitation and emission spectra were recorded with a Jobin–Yvon FluoroMax-4 equipped with a 150-W xenon lamp as the excitation source at room temperature. The lifetime measurements were measured on an Edinburgh Instruments FS920P spectrometer, with a 450-W xenon lamp as the steady-state excitation source at room temperature. Rare earth contents of the complexes were determined by EDTA titration using xylenol orange as an indicator. Elemental analyses (C, H, N) were determined with an Elementar Cario EL elemental analyzer.

3 Results and discussion

3.1 Structure of the ligand and hybrids

As shown in Scheme 1, a two-step route was used to synthesize the ligand 3,4-bis(pyridin-4-ylmethoxy)benzoic acid. Firstly, ethyl 3,4-dihydroxybenzoate was readily obtained by the esterification reaction of commercially available 3,4-dihydroxybenzoic acid with ethanol. Finally, the ligand 3,4-bis(pyridin-4-ylmethoxy)benzoic acid was prepared by NaOH-mediated nucleophilic reaction of ethyl 3,4-dihydroxybenzoate with 4-(chloromethyl)pyridine after acidification. The ligand is designed as the connection between organic rare earth ion complexes and inorganic matrix. The carboxylic acid group of it can react with titanium isopropylate and aluminum isopropylate via ester exchange reaction, while the di-pyridine groups can coordinate with rare earth ions as well as sensitize the luminescence of them. In this way, organic rare earth complexes can be covalently anchored within the network of inorganic–organic hybrid systems. Theoretically, eight-coordination positions of Ln^{3+} (Tb^{3+}, Eu^{3+}) could be occupied by the ligands and water molecules to form an eight-coordination number structure.

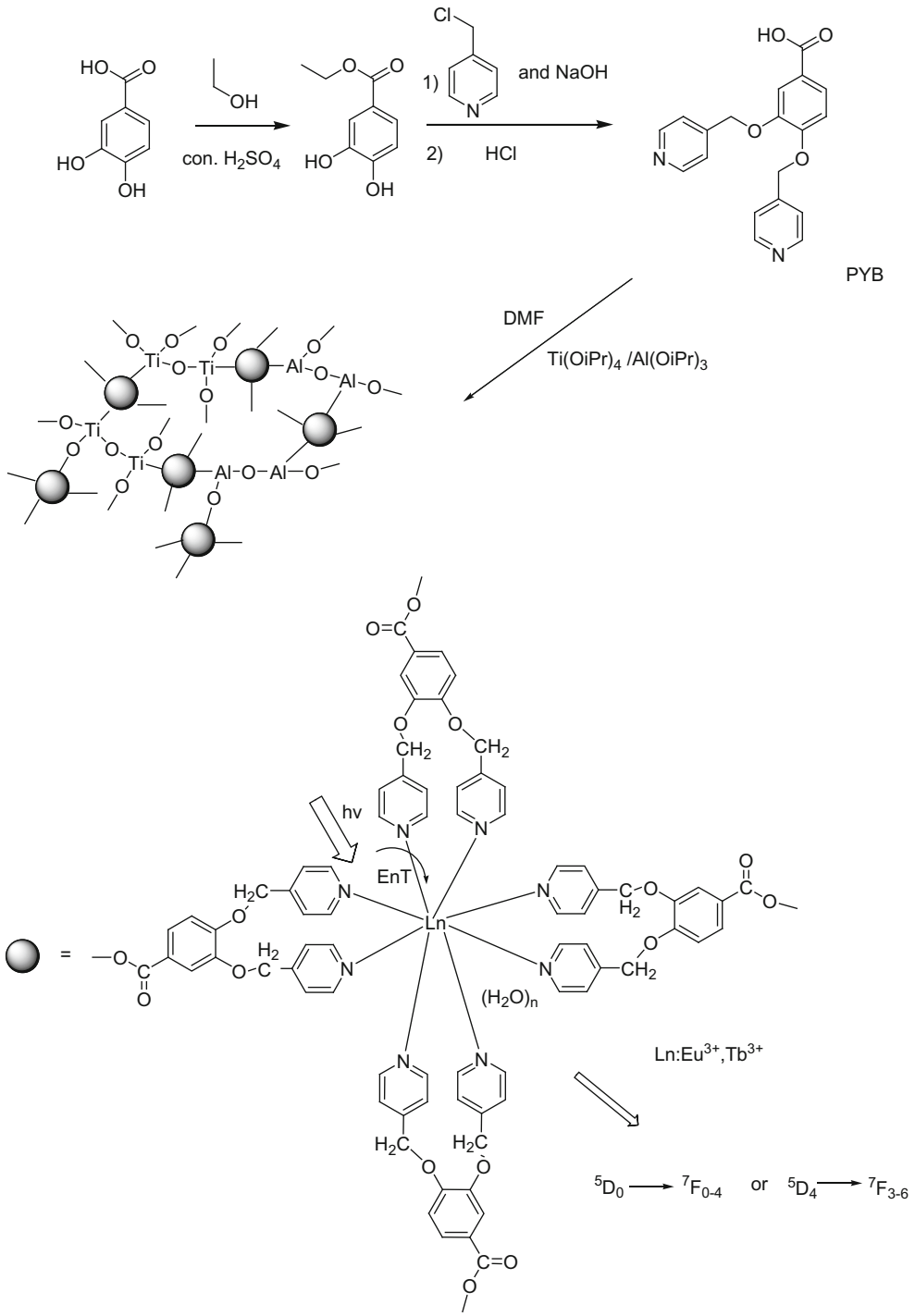

Scheme 1 Synthesis process and predicted structure of the hybrids

3.2 FTIR

The Fourier transform infrared spectra of Al–PYB–Tb, Ti–PYB–Tb and Ti–Al–PYB–Tb hybrids in the 4000–500 cm^{-1} range are shown in Fig. 1, and all the spectra present are almost similar. It is observed that a broad band locates at about 3340 cm^{-1}, which is attributed to ν(O–H) of H_2O molecule in the hybrids. The two peaks at about 3061 and 1603 cm^{-1} correspond to the stretching vibration of C=N in pyridine ring. The peaks located at 1653 cm^{-1} can be assigned to the typical stretching vibration of the carbonyl group, and no absorption bands from the acid can be observed comparing the spectra of PYB, indicating that the corresponding acid was successfully connected to the inorganic

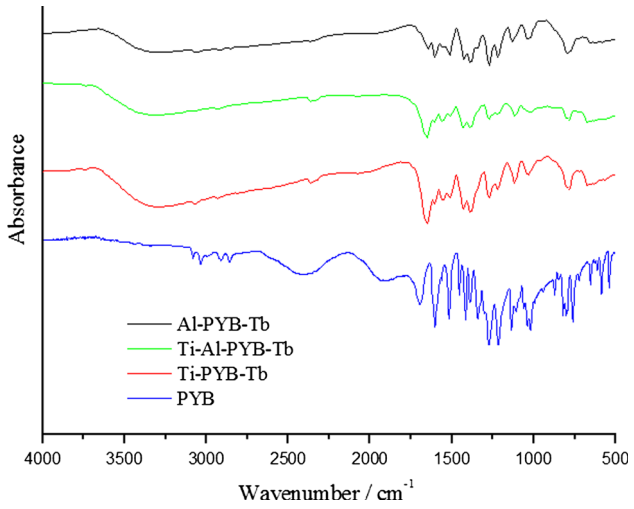

Fig. 1 FTIR spectra of the hybrids containing Tb^{3+} and PYB

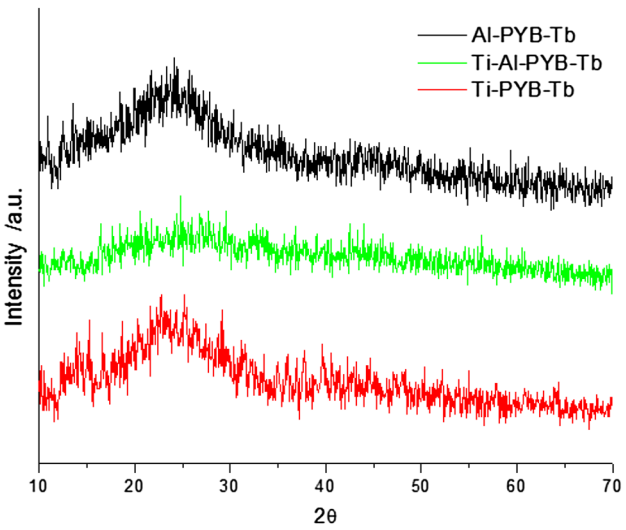

Fig. 2 XRD spectra of the hybrids containing Tb^{3+}

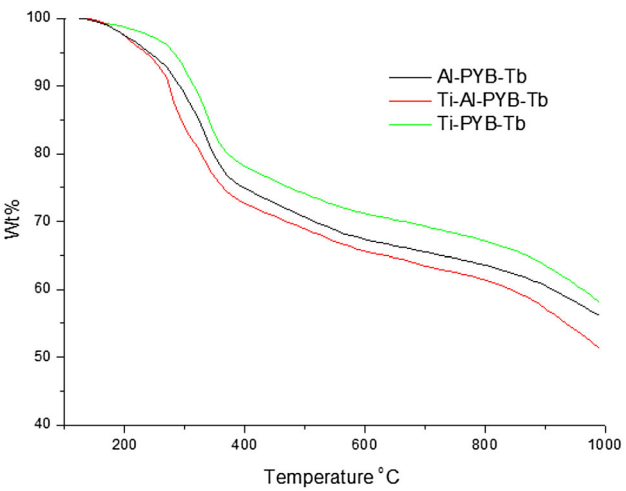

Fig. 3 Thermogravimetry trace of the hybrids containing Tb^{3+}

frameworks. The broad band in the range of 500–991 cm^{-1} has proved the formation of the group Ti–O–Ti, Al–O–Al and Al–O–Ti framework network in the hybrids [20, 21].

3.3 XRD

The diffractograms of the hybrid materials from 10° to 70° presented in Fig. 2 show that all the structures of the hybrids are amorphous or non-periodic at long range. It might be attributed that the inorganic backbones possess less orderliness. The broad peak centered around 23.5° in the XRD patterns of Al–PYB–Tb may be ascribed to the coherent diffraction of the titanic backbone of the hybrids. The structural unit distance, calculated using the Bragg law, is approximately 3.78 Å. In Ti–PYB–Tb system, their broad peaks center at about 24.6° and structural unit distance is about 3.61 Å. In Ti–Al–PYB–Tb system, their broad peaks center at about 23.9° and structural unit distance is about 3.72 Å (Fig. 3).

3.4 TGA

Thermo gravimetric analysis (TGA) is performed on the hybrids in N_2 atmosphere from 100 to 1000 °C. As shown in Fig. 5, it can be observed that these three samples behave the similar change trends in weight loss and three main degradation steps from the TGA curves. The first weight loss procedure about 2–2.5 % before 200 °C can be attributed to the loss of the adsorbed water and residual solvent DMF evaporated. All the curves exhibit sharp weight loss in the temperature from the beginning 200 °C to about 375 °C, and the weight loss is about 17.6 % for Ti–PYB–Tb, 20.5 % for Al–PYB–Tb and 23 % for Ti–Al–PYB–Tb. It is related to the decomposition of terbium complex moieties linking between Tb^{3+} and inorganic matrixes. The last mass loss about 24 % for Ti–PYB–Tb, 22 % for Al–PYB–Tb and 23.7 % for Ti–Al–PYB–Tb is from 375 to 1000 °C, probably corresponding to the decomposition of the residual organic groups covalently bonded to the inorganic matrixes. Comparing the three curves, Ti–PYB–Tb and Al–PYB–Tb possess higher thermal stability than composite Ti–Al–PYB–Tb. Besides, it also reveals that Ti–O–Ti inorganic matrix has more excellent thermal stabilities compared to the other two inorganic matrixes.

3.5 SEM

The transmission electron microscopy is introduced to investigate the morphology of the hybrid materials. The images of the hybrid materials Ti–PYB–Tb, Al–PYB–Tb and Ti–Al–PYB–Tb are given in Fig. 4. The morphology

of hybrids is aggregates of small particles owing to sol–gel procedure. The dimension of the particles is about 0.2–0.5 μm in Ti–PYB–Tb system, while much larger particles in Al–PYB–Tb and Ti–Al–PYB–Tb systems can be observed. There is difference between the three kinds of hybrid materials which may be assigned to the difference of the metallic alkoxide matrix.

3.6 Photophysical properties

The luminescence property of these resulting hybrid materials have been measured at room temperature. As shown in Fig. 5a, the excitation spectra of Tb-containing hybrid materials are obtained by monitoring the emission of Tb^{3+} at 545 nm and dominated by a broad band centered at about 300 nm for these hybrid materials which are ascribed to the characteristic absorption of the rare earth complexes arising from the efficient transition based on pyridine ring. The intensity of the excitation spectrum of Al–PYB–Tb is stronger than that of the other Tb-containing hybrid materials. From the emission spectra in Fig. 6a, the emission lines are assigned to the $^5D_4 \rightarrow {}^7F_J$ transitions located at 489, 542, 583 and 620 nm, for $J = 6$, 5, 4, and 3, respectively, where the most striking green luminescence ($^5D_4 \rightarrow {}^7F_5$) located at 542 nm is observed. The emission intensities of the hybrids are in the order: Al–PYB–Tb > Ti–Al–PYB–Tb > Ti–PYB–Tb, which corresponds to the results of excitation spectra.

The excitation spectra of Eu-containing hybrid materials in Fig. 5b were recorded by monitoring the $^5D_0 \rightarrow {}^7F_2$ transition

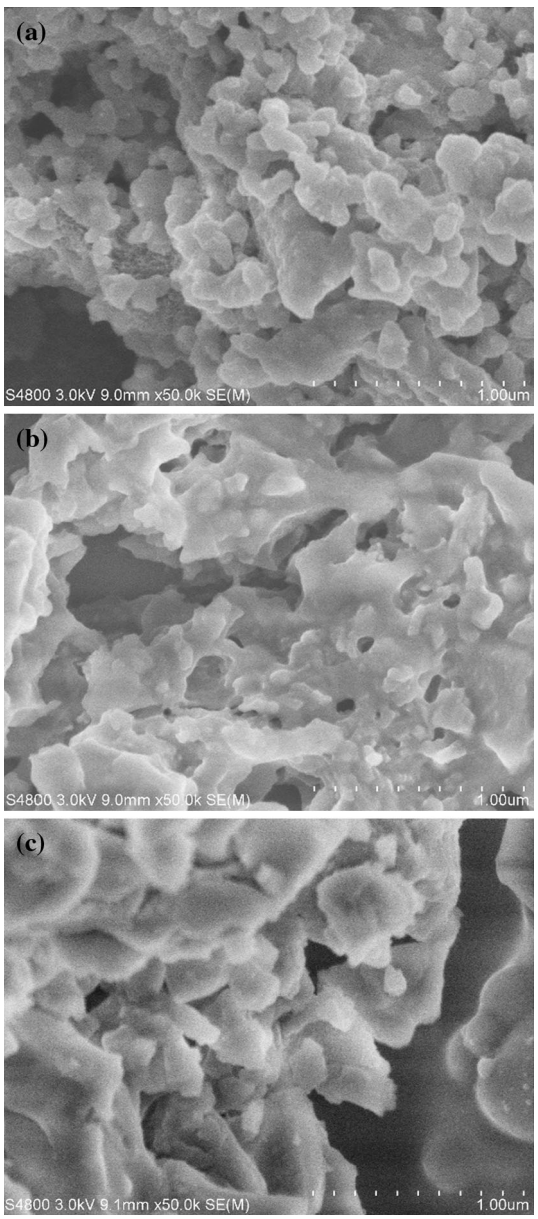

Fig. 4 Selected scanning electron images for the hybrid materials **a** Ti–PYB–Tb, **b** Ti–Al–PYB–Tb, **c** Al–PYB–Tb

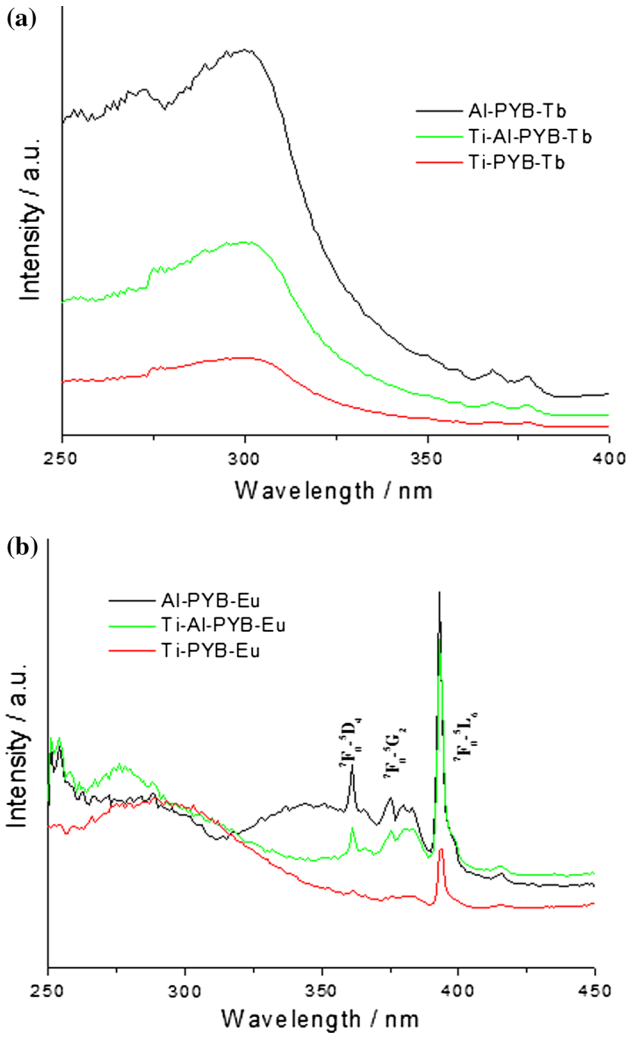

Fig. 5 Excitation spectra of **a** the hybrids containing Tb^{3+} and **b** the hybrids containing Eu^{3+}

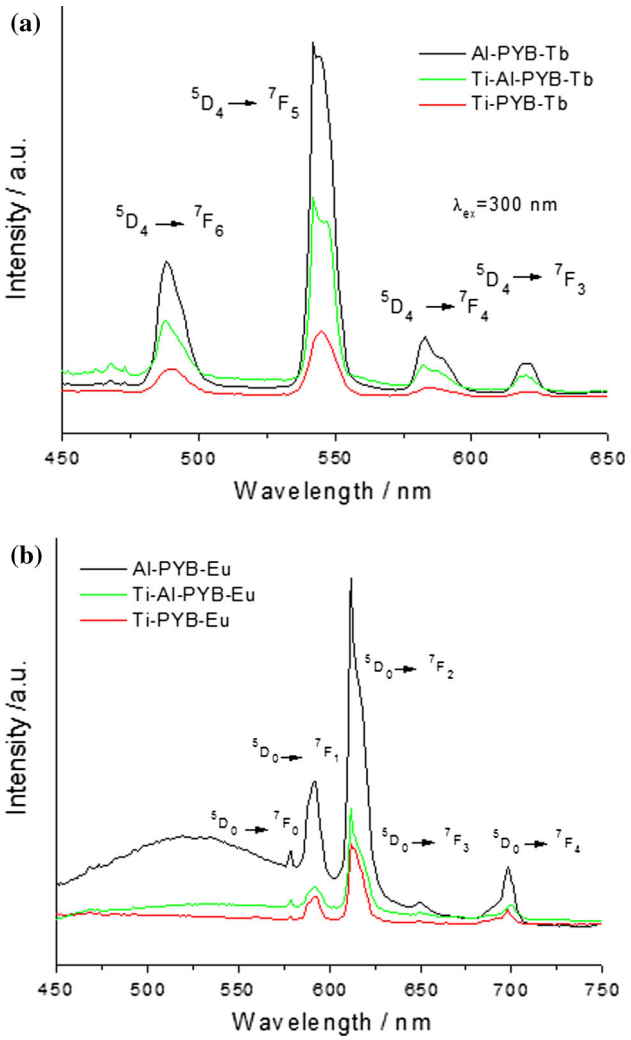

Fig. 6 Emission spectra of **a** the hybrids containing Tb^{3+} and **b** the hybrids containing Eu^{3+}

at 613 nm. The spectra are dominated by a broad excitation band centered at about 250–375 nm in the ultraviolet region. It is assigned to the absorption of the ligands to their π/π^* transition. Transitions at 363, 383 and 394 nm were observed and were attributed to $^7F_0 \rightarrow {}^5D_4$, $^7F_0 \rightarrow {}^5G_2$ and $^7F_0 \rightarrow {}^5L_6$ transitions of Eu^{3+} ion, respectively. The emission luminescence behavior of the Eu-containing hybrid materials has been investigated by the direct excitation of the ligand (293 nm for Ti–PYB–Eu, 276 nm for Ti–Al–PYB–Eu, 282 nm for Al–PYB–Eu). The emission spectra are given in Fig. 6b. It can be clearly observed that characteristic Eu^{3+} ion emission bands in the 450–700 nm range, which are assigned to the $^5D_0 \rightarrow {}^7F_J$ ($J = 0$–4), transition at 578, 590, 613, 650 and 695 nm. Further, the $^5D_0 \rightarrow {}^7F_2$ emission around 613.0 nm is the most predominant transition among these transitions, so the strong red luminescence can be observed in the emission spectra. It is well known that the $^5D_0 \rightarrow {}^7F_2$ transition is a typical electric dipole transition, which is sensitive to the local symmetry of the coordination sphere of Eu^{3+} ions, while $^5D_0 \rightarrow {}^7F_1$ is practically independent of the host material and therefore can be used as internal standard to explain the ligand differences. Moreover, the intensity ratios of the luminescence transitions ($^5D_0 \rightarrow {}^7F_2/{}^5D_0 \rightarrow {}^7F_1$, the red/orange ratio) have been widely taken as an indicator of the local environment of europium ions [22–24].

According to the intensity ratio listed in Table 1, it is concluded that the chemical environment around the Eu^{3+} ions is in low symmetry. The luminescence lifetime decay curves of the hybrid materials are measured at the room temperature, and all of the luminescence decays fit a double-exponential law, suggesting that Tb^{3+} and Eu^{3+} occupy two different environments in the hybrid systems. The resulting average luminescent lifetimes of hybrids are in Table 1. It appears that the lifetimes of Eu-containing hybrid materials are slightly lower than those of Tb-containing hybrid materials.

4 Conclusion

In summary, modifying PYB with alumina and titania gels through the sol–gel process results in the formation of new inorganic/organic rare earth hybrid materials. These obtained materials display connection between organic and inorganic parts on a molecular level, and they are amorphous and heat stabilized. Measurements of the photoluminescent properties show that the final Tb/Eu-containing

Table 1 Intensity ratios of $^5D_0 \rightarrow {}^7F_2/{}^5D_0 \rightarrow {}^7F_1$ and lifetimes of the samples

Sample	$^5D_0 \rightarrow {}^7F_2/{}^5D_0 \rightarrow {}^7F_1$	τ_1^a	τ_2^a	A_1	A_2	τ^b
Al–PYB–Eu	2.81	21.49	145.00	58.11	41.89	123.93
Ti–Al–PYB–Eu	2.59	15.87	51.90	49.95	50.05	43.47
Ti–PYB–Eu	2.68	9.30	27.60	54.48	45.52	22.34
Al–PYB–Tb	_	307.80	212.50	82.45	17.55	295.59
Ti–Al–PYB–Tb	_	227.70	180.70	54.36	45.64	208.9
Ti–PYB–Tb	_	155.80	136.60	80.86	19.14	152.5

[a] The decay curve can be fitted well by $I = I_0 + A_1 \exp(-(t - t_0)/\tau_1) + A_2 \exp(-(t - t_0)/\tau_2)$

[b] Average data obtained according to the equation: $\tau = (A_1\tau_1^2 + A_2\tau_2^2)/(A_1\tau_1 + A_2\tau_2)$

hybrid materials present the typical green and red emissions, respectively, suggesting that organic ligand can efficiently sensitize rare earth ions in the hybrid materials.

Acknowledgments This present work was financially supported by the National Natural Science Foundation of China (Grant Nos. 51272085 and 21171066) and the key technology and equipment of efficient utilization of oil shale resources (No. OSR-05).

References

1. Sabbatini N, Guardigli M, Lehn JM (1993) Luminescent lanthanide complexes as photochemical supramolecular devices. Coord Chem Rev 123:201–228
2. Dirr S, Wiese S, Johannes HH, Ammermann D, Bohler A, Grahn W, Kowalsky W (1997) Luminescence enhancement in microcavity organic multilayer structures. Synth Met 91:53–56
3. Carlos LD, Ferreira RAS, Bermudez VDZ, Ribeiro SJL (2009) Lanthanide-containing light-emitting organic–inorganic hybrids: a bet on the future. Adv Mater 21:509
4. Kido J, Okamoto Y (2002) Organo lanthanide metal complexes for electroluminescent materials. Chem Rev 102:2357
5. Weissman SI (1942) Intramolecular energy transfer the fluorescence of complexes of europium. J Chem Phys 10:214–217
6. Matthews LR, Knobbe ET (1993) Luminescence behavior of europium complexes in sol–gel derived host materials. Chem Mater 5:1697–1700
7. Binnemans K (2009) Lanthanide-based luminescent hybrid materials. Chem Rev 109:4283–4374
8. Carlos LD, Ferreira RAS, Bermudez VD (2011) Progress on lanthanide-based organic–inorganic hybrid phosphors. Chem Soc Rev 40:536–554
9. Harreld JHA, Esaki G, Stucky D (2003) Low-shrinkage, high hardness, and transparent hybrid coatings: poly(methyl methacrylate) cross-linked with silsesquioxane. Chem Mater 15:3481–3489
10. Sanchez C, Soler-Illia GJDA, Ribot F, Lalot T, Mayer CR, Cabuil V (2001) Designed hybrid organic-inorganic nanocomposites from functional nanobuilding blocks. Chem Mater 13:3061–3083
11. Tanner PA, Yan B, Zhang HJ (2000) Preparation and luminescence properties of sol–gel hybrid materials incorporated with europium complexes. J Mater Sci 35:4325
12. Koslova NI, Viana B, Sanchez C (1993) Rare-earth-doped hybrid siloxane-oxide coatings with luminescent properties. J Mater Chem 3:111
13. Viana B, Koslova N, Aschehoug P, Sanchez C (1999) Optical properties of neodymium and dysprosium doped hybrid siloxaneoxide coatings. J Mater Chem 5:719–722
14. Choi J, Tamaki R, Kim SG, Laine RM (2003) Organic/inorganic imide nanocomposites from aminophenylsilsesquioxanes. Chem Mater 15:3365
15. Franville AC, Zambon D, Mahiou R (2000) Luminescence behavior of sol–gel-derived hybrid materials resulting from covalent grafting of a chromophore unit to different organically modified alkoxysilanes. Chem Mater 12:428–435
16. Li HR, Liu P, Wang YG, Zhang L, Yu JB, Zhang HJ, Liu BY, Schubert U (2009) Preparation and luminescence properties of hybrid titania immobilized with lanthanide complexes. J Phys Chem C 113:3945–3949
17. Cuan J, Yan B (2014) Luminescent lanthanide-polyoxometalates assembling zirconia–alumina–titania hybrid xerogels through task-specified ionic liquid linkage. RSC Adv 4:1735–1743
18. Zhang Q, Sheng Y, Zheng KY, Qin XM, Ma PC, Zou HF (2015) Novel luminescent lanthanide complexes assembling alumina/titania/silica hybrids through 2-phenylmalonic acid linkage. J Non-Cryst Solids 413:34–38
19. Yan B, Li YJ (2011) Photoactive lanthanide (Eu^{3+}, Tb^{3+}) centered hybrid systems with titania (alumina)-mesoporous silica based hosts. J Mater Chem 21:18454–18461
20. Saif M, Abdel-Mottaleb MSA (2008) Titanium dioxide nanomaterial doped with trivalent lanthanide ions of Tb, Eu and Sm: preparation, characterization and potential applications. Inorg Chim Acta 360:2863–2874
21. de Faria EH, Ciuffi KJ, Nassar EJ, Vicente MA, Trujillano R, Calefi PS (2010) Novel reactive amino-compound: tris(hydroxymethyl)aminomethane covalently grafted on kaolinite. Appl Clay Sci 48:516–521
22. Soares-Santos PCR, Nogueira HIS, Félix V, Drew MGB, Ferreira RAS, Carlos LD, Trindade T (2003) Novel lanthanide luminescent materials based on complexes of 3-hydroxypicolinic acid and silica nanoparticles. Chem Mater 15:100
23. Teotonio ES, Espínola JGP, Brito HF, Malta OL, Oliveria SF, de Foria DLA, Izumi CMS (2002) Influence of the *N*-[methylpyridyl] acetamide ligands on the photoluminescent properties of Eu(III)-perchlorate complexes. Polyhedron 21:1837
24. Li Y, Guo M, Yan B (2012) Photoluminescent Eu^{3+}/Tb^{3+} hybrids from the copolymerization of organically modified silane. Colloid Polym Sci 290:1765–1775